Modal Power Distribution in Ducts at High Frequencies

S. M. Baxter* and C. L. Morfey†
University of Southampton, Southampton, England

Sound attenuation in a lined duct depends on, among other factors, the distribution of power among the propagating modes. Up to now, the modal power distribution has not in general been measurable because existing measurement techniques have involved resolving for all the modes cut on at a given frequency. At high frequencies such techniques become impractical. In this paper, new theoretical results are given about the high-frequency asymptotic behavior of duct sound fields. The results are based on a description in which the power distribution is treated as a continuous function of modal coordinates. The results lead to a new experimental technique for investigating the power distribution. A finite set of cross-spectral density measurements is used to estimate the distribution as a function of modal coordinates. The finite amount of data provides a limit to the modal resolution of the estimate, rather than a limit to the number of modes to be considered. Results from such an experiment are given and discussed.

Nomenclature

A_{mn} = complex modal amplitude
a,b = lengths of sides of rectangular duct
B_{mn} = modal pressure spectrum
$C(r)$ = normalized CCSD
c_0 = equilibrium sound speed
E = ensemble average operator
$F(v,u)$ = function occurring in Fourier representation of $p(x)$
$f(\theta,\phi)$ = arbitrary function of angle
$I(v,u)$ = plane-wave weighting function
$I_{lq}, \hat{I}_{lq}$ = spherical harmonic coefficients
i = $(-1)^{\frac{1}{2}}$
$J_l(x)$ = Bessel function, order l
$j_l(x)$ = spherical Bessel function, order l
K_{lq} = spherical harmonic coefficient
$\mathbf{k}, \mathbf{k}_1, \mathbf{k}_2, \mathbf{k}_3, \mathbf{k}_4$ = wavenumber vectors
k = $|\mathbf{k}| = \omega/c_0$
M = number of microphone positions
N = number of terms in fitting series
$P_l(x)$ = Legendre polynomial, order l
$p(\mathbf{x})$ = pressure Fourier transformed with respect to time
R = residual error
R_{norm} = normalized R
r = $\mathbf{x}-\mathbf{x}'$
r = radial distance
$S_N(r)$ = sum of N harmonics
u,u' = azimuthal spherical angles
v,v' = polar spherical angles
W_{mn} = modal power spectrum
$W(v,u)$ = modal power function
$w(\theta_j)$ = weighting function
$\mathbf{x},\mathbf{x}'$ = position vectors
x,y,z = Cartesian coordinates
$Y_l^q(v,u)$ = normalized spherical harmonic
θ = polar spherical angle
ρ_0 = equilibrium density
τ_{mn} = normalized axial wavenumber
ϕ = azimuthal spherical angle
$\psi_{mn}(x)$ = modal pressure distribution
ω = radian frequency

Superscript

$(\ )^*$ = complex conjugate

Subscripts

j = value at microphone position j
l,q = integer suffixes for spherical harmonics
m,n = integer suffixes for modes

Presented as Paper 81-2013 at the AIAA 7th Aeroacoustics Conference, Palo Alto, Calif., Oct. 5-7, 1981; submitted Oct. 16, 1981; revision received April 12, 1982.

*Research Student, Institute of Sound and Vibration Research.
†Senior Lecturer, Institute of Sound and Vibration Research. Member AIAA.

I. Introduction

SOUND attenuation in a lined duct depends not only on the geometry of the duct and the properties of the liner, but also on the distribution of power among the cut-on (propagating) modes. A common experimental method for assessing the way a given liner attenuates propagating sound is to measure the drop in sound pressure level between the ends of a lined duct. If the input modal power distribution is unknown, the results of such an experiment are ambiguous, in the sense that a wide range of liner properties could have produced the same attenuation. Furthermore, if an assumed modal power distribution is used in interpreting such measurements, different values of the liner properties may be inferred from different rigs, since the actual power distribution in a given rig may be different from the assumed distribution.

Up to now, the modal power distribution in ducts at high frequencies has not in general been measurable, because existing techniques have involved resolving for all the modes cut on at a given frequency. This requires that the number of experimental observations be comparable to the number of cut-on modes. The number of cut-on modes increases roughly as the square of the frequency, and at high frequencies there can be so many cut-on modes that such techniques are impractical.

The motivation for the present work is the need to design a new experimental technique for assessing a duct's modal power distribution. The technique is intended to work at high frequencies, when the number of cut-on modes is much greater than the number of experimental observations.

The technique stems from new theoretical results described in the next section of the paper, concerning the high-frequency behavior of a sound field in a duct. The theory is based on a statistical description in which the power distribution is treated as a continuous function of modal

coordinates. Using these results, an estimate of the modal power distribution can be obtained from experimental measurements of spectral densities in the duct. The estimate of the distribution is smoothed over many modes, rather than being a mode-by-mode weighting. The fact that the number of experimental observations is limited is reflected in a limit to the modal resolution of the estimate, rather than as a limit to the number of modes to be considered.

An outline of the new theoretical results is given in the next section. The following section is a description of the practical implementation of the results. Finally, results from an illustrative microphone traverse experiment are given and discussed.

II. Theory

The theoretical approach used here is based on techniques applied by earlier workers to analogous problems in architectural acoustics. The central idea is that, with increasing frequency, the many-mode sound field in an enclosure (a duct or a room) can approach an asymptotic form known as a free-wave sound field.[1] The experimental method is to study the properties of the asymptotic field and hence to draw conclusions about the underlying modal field.

The main steps in the theoretical argument are sketched below; further details are available in Ref. 2.

A. Free-Wave Fields and Duct Mode Fields

The starting point of the theory is to regard a duct sound field as being composed of plane waves. Every sound field made up of propagating waves can be regarded as a weighted sum of plane waves. This is expressed by the field's spatial Fourier representation[3]:

$$p(\boldsymbol{x}) = \int_0^{2\pi} du \int_0^{\pi} dv \, \sin v \; F(v,u) \exp(i\boldsymbol{k}\cdot\boldsymbol{x}) \tag{1}$$

The spherical angles u and v determine the direction of the wavenumber vector $\boldsymbol{k}$. The integrals are taken over real angles.

The spatial complex cross-spectral density (CCSD) of the field, which is a typical second-order statistic of the field, can be defined by

$$\mathrm{CCSD}(\boldsymbol{x},\boldsymbol{x}') = E[p(\boldsymbol{x})p^*(\boldsymbol{x}')] \tag{2}$$

and the field's power spectral density (PSD) can be defined by

$$\mathrm{PSD}(\boldsymbol{x}) = E[\,|p(\boldsymbol{x})|^2] \tag{3}$$

It is convenient also to define a normalized CCSD, C, by

$$C(\boldsymbol{x},\boldsymbol{x}') = \mathrm{CCSD}(\boldsymbol{x},\boldsymbol{x}') / [\mathrm{PSD}(\boldsymbol{x})\,\mathrm{PSD}(\boldsymbol{x}')]^{1/2} \tag{4}$$

A free-wave field is, by definition, made up of uncorrelated plane waves propagating in different directions. If the field is free wave, then expressions for such second-order statistics as the CCSD—obtained by substituting Eq. (1) into Eq. (2)—collapse to simple weighted sums of plane waves:

$$\mathrm{CCSD}(\boldsymbol{r}) = \iint du \; dv \; \sin v \; I(v,u) \exp(i\boldsymbol{k}\cdot\boldsymbol{r}) \tag{5}$$

It can be seen that a free-wave field is spatially homogeneous: that is, the field's second-order statistics depend only on the separation vector $\boldsymbol{r}$. The weighting function $I(v,u)$ is a measure of the angular dependence of intensity in the field, and can be estimated experimentally[4,5] from measurements of the CCSD.

Previous workers in the field of architectural acoustics[6] have found that, if certain conditions are satisfied, the many-mode field in a rectangular room approaches a free-wave form asymptotically with increasing frequency. The main new conclusion of the present work is that, if certain conditions are satisfied, the many-mode field in a rectangular or circular hard-walled duct can also approach a free-wave form at high frequencies. This is proved by showing that the field's second-order statistics, for example, the CCSD, approach the homogeneous form of Eq. (5) at high frequency (see Sec. II.B.). Further, the plane-wave weighting function $I(v,u)$ of Eq. (5) turns out to be related to the duct's modal power distribution.

The important consequence of this result is that an estimate of the modal power distribution at high frequency can be obtained from an estimate of the function $I(v,u)$, which in turn can be derived from CCSD measurements. These are obtained experimentally using a pair of microphones in the duct. Thus a method can be developed for deriving experimentally the modal power distribution in ducts at high frequencies.

B. Method of Proof: Rectangular Duct

This section is an illustrative outline of the method used to establish the aforementioned result for a duct with a rectangular cross section. The method of proof is similar to that used by Morrow[6] to solve the analogous problem of a high-frequency sound field in a rectangular, hard-walled room. The proof for a circular duct is similar in form but more complicated in detail.[2]

Let Cartesian axes be defined in the rectangular duct so that the duct has its axis parallel to the z axis and its sides at $x=0,a$ and $y=0,b$. The pressure in the duct is given by

$$p(\boldsymbol{x}) = \sum_m \sum_n A_{mn} \psi_{mn}(\boldsymbol{x}) \tag{6}$$

with $\psi_{mn}(\boldsymbol{x})$ a modal pressure distribution, and the sum being taken over cut-on modes only.

The modal function ψ_{mn} is given by

$$\psi_{mn}(\boldsymbol{x}) = \cos(m\pi x/a)\cos(n\pi y/b)\exp(ik\tau_{mn}z) \tag{7}$$

Here τ_{mn} is the mode's normalized axial wavenumber, and

$$(m\pi/a)^2 + (n\pi/b)^2 + (k\tau_{mn})^2 = k^2 \tag{8}$$

The restriction to cut-on modes implies that τ_{mn} is real.

$\psi_{mn}(\boldsymbol{x})$ can also be expressed as a sum of four plane waves:

$$\psi_{mn}(\boldsymbol{x}) = \tfrac{1}{4}[\exp(i\boldsymbol{k}_1\cdot\boldsymbol{x}) + \exp(i\boldsymbol{k}_2\cdot\boldsymbol{x}) + \exp(i\boldsymbol{k}_3\cdot\boldsymbol{x}) + \exp(i\boldsymbol{k}_4\cdot\boldsymbol{x})] \tag{9}$$

where

$$\boldsymbol{k}_1 = (m\pi/a, n\pi/b, k\tau_{mn}) \tag{10a}$$

$$\boldsymbol{k}_2 = (-m\pi/a, n\pi/b, k\tau_{mn}) \tag{10b}$$

$$\boldsymbol{k}_3 = (m\pi/a, -n\pi/b, k\tau_{mn}) \tag{10c}$$

$$\boldsymbol{k}_4 = (-m\pi/a, -n\pi/b, k\tau_{mn}) \tag{10d}$$

If Eq. (9) is substituted into Eq. (6), an expression for $p(\boldsymbol{x})$ as a sum of plane waves can be derived [cf. Eq. (1)]:

$$p(\boldsymbol{x}) = \tfrac{1}{4} \sum_m \sum_n A_{mn} [\exp(i\boldsymbol{k}_1\cdot\boldsymbol{x}) + \exp(i\boldsymbol{k}_2\cdot\boldsymbol{x}) + \exp(i\boldsymbol{k}_3\cdot\boldsymbol{x}) + \exp(i\boldsymbol{k}_4\cdot\boldsymbol{x})] \tag{11}$$

It is now assumed that the following conditions are satisfied:

1) The modes are uncorrelated.

2) The frequency is high enough and the modal weighting smooth enough for modal sums to be approximated by integrals in which m, n are treated as continuous variables.

An expression for the field's CCSD can be derived by substituting Eq. (11) into Eq. (2). This complicated expression is simplified by the use of assumption 1. Further, if the two observation positions x, x' are close together and far from the walls of the duct, then at high frequency the dominant part of the CCSD expression can be shown to be[2]

$$\mathrm{CCSD}(x,x') = \frac{1}{16}\sum_m\sum_n B_{mn}[\exp(ik_1\cdot r)+\exp(ik_2\cdot r) + \exp(ik_3\cdot r)+\exp(ik_4\cdot r)] \tag{12}$$

where

$$B_{mn} = E(|A_{mn}|^2) \tag{13}$$

is the modal pressure spectrum. B_{mn} is related to the modal power W_{mn} by

$$W_{mn} = -\tfrac{1}{8}B_{mn}(\tau_{mn}ab/\rho_0 c_0) \tag{14}$$

According to assumption 2, the double summation in Eq. (12) can be converted into a double integral over continuous m and n. The integration variables are next converted from m, n to the azimuthal and polar spherical angles u, v by the following transformation:

$$m = (k/\pi)\sin v\ \cos u \tag{15a}$$

$$n = (kb/\pi a)\sin v\ \sin u \tag{15b}$$

$$\tau_{mn} = \cos v \tag{15c}$$

The power function W_{mn} may then be regarded as a continuous function $W(v,u)$ of v and u.

Since m and n are both taken as positive, the range of v is 0 to π, and the range of u is 0 to $\pi/2$. The range of u, however, can be extended up to 2π by extending the definition of $W(v,u)$ as follows:

$$W(v,u) = W(v,\pi-u) \text{ when } \pi/2<u\le\pi \tag{16a}$$

$$W(v,u) = W(v,u-\pi) \text{ when } \pi<u\le 3\pi/2 \tag{16b}$$

$$W(v,u) = W(v,2\pi-u) \text{ when } 3\pi/2<u<2\pi \tag{16c}$$

Then, after some manipulation, the double summation on the right of Eq. (12) can be replaced by a double integral over v and u:

$$\mathrm{CCSD}(r) = \int_0^{2\pi} du \int_0^{\pi} dv \sin v\,(-k^2\rho_0 c_0/2\pi^2) \times W(v,u)\exp(ik\cdot r) \tag{17}$$

This has the same form as the free-wave field CCSD expression of Eq. (5), with the plane-wave weighting function $I(v,u)$ given by

$$I(v,u) = (-k^2\rho_0 c_0/2\pi^2)\,W(v,u) \tag{18}$$

Thus it has been proven that, if the mode field in a hard-walled, rectangular duct satisfies conditions 1 and 2, it approaches a free-wave field form at high frequency, and the plane-wave weighting function I characterizing the free-wave field is related to the modal power distribution by Eq. (18).

C. Result for Circular Duct

Similarly, it can be proven that if the mode field in a hard-walled, circular duct satisfies conditions 1 and 2, and also a further necessary condition:

3) The modal power distribution at any frequency is a function only of modal cut-off frequency (i.e., of axial wavenumber, then the mode field approaches a free-wave field form at high frequency. The modal power distribution in such a field depends only on a polar spherical angle v, which is related to axial wavenumber by Eq. (15c). The plane-wave weighting function I is found to be

$$I(v) = (-k^2\rho_0 c_0/2\pi^2)\,W(v) \tag{19}$$

which should be compared with Eq. (18), derived for the rectangular duct.

D. Semidiffuse Fields

This section is a brief description of important special cases of the preceding results.

If all the propagating modes in a rectangular or circular duct carry equal power, and the duct has a nonreflecting termination, it is straightforward to show that

$$W(v,u) = \text{const} \qquad 0\le v<\pi/2 \tag{20a}$$

$$W(v,u) = 0 \qquad \pi/2<v\le\pi \tag{20b}$$

It then follows from Eqs. (18) and (19) that I has the same angular dependence as W, and the resulting field is called "semidiffuse."[7] (See the Appendix).

A semidiffuse field has a plane-wave weighting that is uniform over a half-space. A diffuse field[8] has a plane-wave weighting that is uniform over all angles. A comparable result, obtained by workers in architectural acoustics,[6] is that if the modes in a rectangular, hard-walled room have equal mean energy, the resulting high-frequency free-wave field is diffuse.

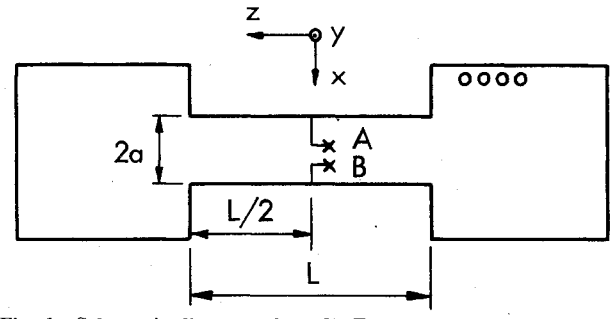

Fig. 1 Schematic diagram of the NTF. The y axis is vertical, the x and z axes horizontal. a = 34.29 cm; L = 2.032 m; o = Hartmann generator; × = microphone diaphragm.

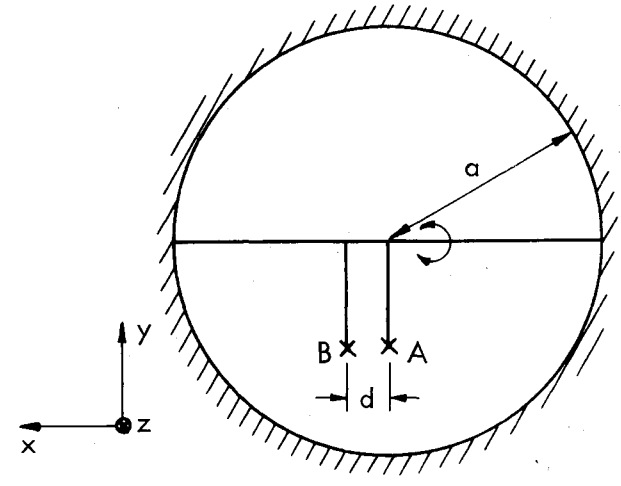

Fig. 2 Schematic diagram of microphone arrangement in test duct. a = 34.29 cm; d = 2.54 cm; × = microphone diaphragm; arrow shows freedom of movement of microphone A.

III. Practical Implementation

These results lead to an experimental method for determining the modal power distribution. The technique is to estimate the function I from a finite number of CCSD measurements, and hence to estimate the modal power distribution as a function of modal coordinates, via Eq. (18) or Eq. (19). The finite number of data available from such an experiment provides a limit to the modal resolution of the estimate of the power distribution, rather than a limit to the number of cut-on modes to be considered.

Equation (5) is the basis of the technique used to estimate the function I from two-microphone measurements. Let the expansion of I in normalized spherical harmonics[9] be

$$I(v,u) = \sum_{l=0}^{\infty} \sum_{q=-l}^{l} I_{lq} Y_l^q(v,u) \tag{21}$$

(Note that $I_{l-q} = I_{lq}^*$.) Substitution of Eq. (21) into Eq. (5) leads, via standard results,[5,9] to the following expansion for the normalized CCSD:

$$C(r) = \sum_{l=0}^{\infty} \sum_{q=-l}^{l} 4\pi i^l \hat{I}_{lq} j_l(kr)\, Y_l^q(\theta,\phi) \tag{22}$$

Here (r,θ,ϕ) is the expression for r in spherical polar coordinates. A "normalized" weighting function $\hat{I}(v,u)$ is defined by

$$\hat{I}(v,u) = I(v,u)/\text{PSD} \tag{23}$$

with corresponding spherical harmonic coefficients $\hat{I}_{lq}$. The PSD is taken to be uniform, since this is a property of the asymptotic free-wave field.

The procedure now is to use Eq. (22) to estimate some of the coefficients $\hat{I}_{lq}$ by a least-squares fit to experimental data for $C(r)$, and to reconstruct the function $\hat{I}$ by using Eq. (21). Let $C(r)$ be approximated by a suitably chosen set of N terms:

$$S_N(r) = \sum_{l}^{N} \sum_{q} 4\pi i^l K_{lq} j_l(kr)\, Y_l^q(\theta,\phi) \tag{24}$$

Suppose the field is sampled at M $(>N)$ pairs of microphone positions, with vectors r_j $(j=1$ to $M)$. Then the coefficients $\hat{I}_{lq}$ can be estimated by minimizing the sum of squares

$$R = \sum_{j=1}^{M} |C(r_j) - S_N(r_j)|^2 w(\theta_j) \tag{25}$$

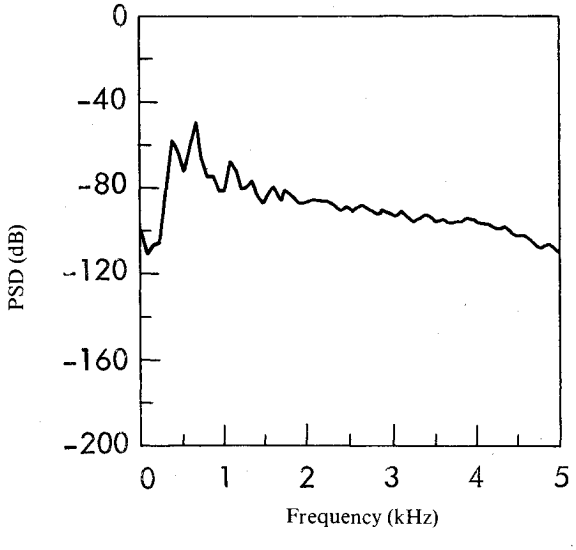

Fig. 3 PSD recorded by microphone A at sampling position 1 (see Table 1). The dB scale is relative; OASPL is about 155 dB.

with respect to the set K_{lq}. The weights $w(\theta_j)$ are given by

$$w(\theta_j) = \tfrac{1}{2}(\cos\theta_2 - \cos\theta_1), \qquad j=1 \tag{26a}$$

$$w(\theta_j) = \tfrac{1}{2}(\cos\theta_{j+1} - \cos\theta_j), \qquad j \neq 1, M \tag{26b}$$

$$w(\theta_j) = \tfrac{1}{2}(\cos\theta_M - \cos\theta_{M-1}), \qquad j=M \tag{26c}$$

Here the vectors r_j are ordered so that $\cos\theta_j < \cos\theta_{j+1}$, for $j=1$ to $M-1$. The weights are a linear approximation to the $\sin\theta$ weighting factor in solid angle integrals of the form

$$\int_0^{2\pi} d\phi \int_0^{\pi} d\theta\, \sin\theta\, f(\theta,\phi) \tag{27}$$

for an arbitrary function f.

The sum of squares is minimized when the coefficients K_{lq} satisfy a certain matrix equation; this can be solved to obtain the minimizing values of the coefficients. The minimizing value of K_{lq} is an estimate of the value of the true spherical harmonic coefficient $\hat{I}_{lq}$.

IV. Description of Experiment

An experiment along the lines described above was performed using the Noise Test Facility (NTF) of the National Gas Turbine Establishment, Farnborough, England. The NTF is a large-scale duct absorber test rig (see Fig. 1). The working section of hard-walled duct used for the experiment is circular, with radius 34.29 cm and length 2.032 m (about 3 diameters). The duct is excited by an inlet from a 5 m × 5 m × 5 m reverberation chamber, within which are four Hartmann generators with peak frequencies of 400, 500, 600, and 750 Hz. The generators are placed so that the duct inlet is not in their direct sound field, and they give an overall sound pressure level in the source reverberation chamber of about 155 dB. The duct leads via an adaptor to a second 5 m × 5 m × 5 m reverberation chamber.

A. Microphone Geometry

Figure 2 shows schematically the two microphones used in the experiment. The microphones were 6.35 mm (¼ in.) Brüel and Kjaer type 4135. They were attached to a traverse rod that stretched across a horizontal diameter of the duct. The traverse rod was at the midsection of the duct. The microphones were attached with their axes perpendicular to the traverse rod, so that their diaphragms were offset from the rod axis. The arrow in the figure indicates the freedom of movement of microphone A on its traverse gear; its diaphragm moved in a circular path about the rod axis.

Microphone A was moved to 12 different positions, whereas B was kept stationary, with its diaphragm pointing toward the source reverberation chamber. The sound field was recorded for 60 s at each position. The position vector of A relative to B for each position is given in Table 1.

Note that the maximum microphone separation of 11.4 cm is roughly one wavelength at 3 kHz. Scattering by the microphones and their support gear was assumed to be negligible at each position.

B. Data Analysis

Analysis of the data was performed using the Data Analysis Centre of the Institute of Sound and Vibration Research at Southampton University. The data were passed through a pair of anti-aliasing filters, with cut-off frequency 5 kHz, and then sampled at a rate of 17,900 samples/s. A total of 25,000 samples was taken from each microphone recording, at each of the 12 positions. Spectral densities were formed using an overlapping segment averaging fast Fourier transform (FFT) technique. A Parzen window was used with a resolution

bandwidth of 69.53 Hz, and enough segments were used to give 388 degrees of freedom.

Typical results are shown in Figs. 3 and 4. Figure 4 is a plot of the normalized CCSD $C(r)$ in modulus and phase form for a particular separation vector r.

The normalized CCSD that would be obtained in an ideal semidiffuse field (with statistical errors, etc., absent) can be computed. (See the Appendix.) Included in Fig. 4 for comparison are modulus and phase plots of normalized CCSD that would be obtained in an ideal semidiffuse field with the same separation vector r as for the experimental results.

C. Computation

A least-squares fit procedure of the type described previously was applied to a set of actual CCSD input data from the experiment and also to a set of synthesized data. The set of input data from the experiment was the set of complex values of normalized CCSD at 3 kHz read off for each of the 12 sampling positions. The synthesized input data were the values of normalized CCSD at 3 kHz that would be observed in a semidiffuse field with the 12 sampling positions used in the real experiment. These CCSD values were obtained numerically using an integral expression for the normalized CCSD in a semidiffuse field (see appendix). The purpose of using a set of synthesized input data was to test the least-squares fit procedure on a case in which the coefficients in the expansion of C[Eq. (22)] are known.

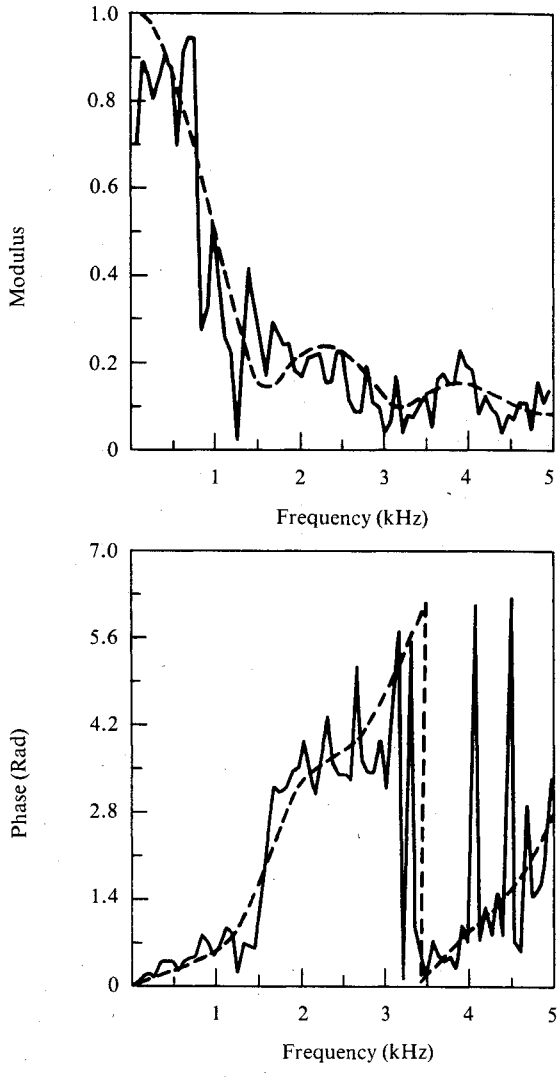

Fig. 4 Modulus and phase of normalized CCSD observed at sampling position 7 (see Table 1). The principal value of phase is shown.

As a preliminary exercise, two simple choices of terms to form the fitting series S_N [see Eq. (24)] were made: 1) the N lowest-order terms, for $N=2, 4, 8$ (these results are given in Tables 2 and 3); 2) the N lowest-order axisymmetric terms (i.e., terms independent of ϕ), for $N=2, 4, 8, 12$ (these results are given in Tables 4 and 5). For each choice of N terms, $N/2$ terms with l even and $N/2$ terms with l odd were chosen. The normalized residual error given in the tables is defined by

$$R_{\text{norm}} = \sum_{j=1}^{M} |C(r_j) - S_N(r_j)|^2 w(\theta_j) \Big/ \sum_{j=1}^{M} |C(r_j)|^2 w(\theta_j) \quad (28)$$

Table 1 Position vectors of the diaphragm of microphone A relative to the diaphragm of microphone B in the coordinate system defined in Figs. 1 and 2

Position No.	r, cm	θ, rad	ϕ, rad
1	2.540	1.571	3.142
2	3.169	1.464	2.509
3	4.335	1.384	2.210
4	5.478	1.328	2.069
5	6.933	1.267	1.965
6	8.921	1.191	1.882
7	11.405	1.099	1.824
8	3.710	1.593	3.958
9	5.010	1.552	4.176
10	6.198	1.511	4.289
11	7.427	1.469	4.362
12	10.167	1.373	4.455

Table 2 Optimal coefficients given by least-squares fitting of low-order terms to synthesized semidiffuse field data

	Number of terms in fitting series S_N 2	4	8	Correct values
1) l odd terms				
K_{10}	0.2108	0.2355	0.1619	0.2443
Re K_{11}	—	−0.0038	−0.0041	0
Im K_{11}	—	−0.0030	0.0058	0
K_{30}	—	—	−0.1074	−0.0933
Re K_{31}	—	—	0.1522	0
Im K_{31}	—	—	0.0296	0
2) l even terms				
K_{20}	0	0	-1×10^{-8}	0
Re K_{21}	—	1×10^{-8}	-6×10^{-8}	0
Im K_{21}	—	0	0	0
Re K_{22}	—	—	0	0
Im K_{22}	—	—	1×10^{-8}	0
K_{40}	—	—	0	0
Error	0.2612	0.2558	0.00004	

Table 3 Optimal coefficients given by least-squares fitting of low-order terms to experimental data

	Number of terms in fitting series S_N 2	4	8
1) l odd terms			
K_{10}	0.0981	0.1195	−0.2453
Re K_{11}	—	−0.0203	−0.0546
Im K_{11}	—	0.0100	0.0260
K_{30}	—	—	−0.2554
Re K_{31}	—	—	1.0456
Im K_{31}	—	—	0.2973
2) l even terms			
K_{20}	0.1077	0.0994	0.3051
Re K_{21}	—	−0.1441	0.9656
Im K_{21}	—	0.0834	−0.0077
Re K_{22}	—	—	0.0801
Im K_{22}	—	—	−0.1222
K_{40}	—	—	0.1565
Error	0.3282	0.1790	0.0807

Table 4 Optimal coefficients given by least-squares fitting of axisymmetric terms to synthesized semidiffuse field data

	Number of terms in fitting series S_N				Correct values
	2	4	8	12	
1) l odd terms					
K_{10}	0.2108	0.2270	0.2442	0.2443	0.2443
K_{30}	—	−0.0712	−0.0930	−0.0933	−0.0933
K_{50}	—	—	0.0569	0.0585	0.0585
K_{70}	—	—	−0.0343	−0.0426	−0.0427
K_{90}	—	—	—	0.0337	0.0336
K_{110}	—	—	—	−0.0322	−0.0277
2) l even terms					
K_{20}	0	0	0	0	0
K_{40}	—	0	0	-2×10^{-8}	0
K_{60}	—	—	-4×10^{-8}	5.3×10^{-7}	0
K_{80}	—	—	2.1×10^{-7}	8.5×10^{-6}	0
K_{100}	—	—	—	1.1×10^{-4}	0
K_{120}	—	—	—	-6.9×10^{-4}	0
Error	0.2612	0.0032	3×10^{-8}	0	

Table 5 Optimal coefficients given by least-squares fitting of axisymmetric terms to experimental data

	Number of terms in fitting series S_N			
	2	4	8	12
1) l odd terms				
K_{10}	0.0981	0.0977	0.1075	0.0370
K_{30}	—	0.0015	0.0031	0.0046
K_{50}	—	—	0.0096	0.4573
K_{70}	—	—	−0.3365	2.903
K_{90}	—	—	—	−194.4
K_{110}	—	—	—	2533.0
2) l even terms				
K_{20}	0.1077	0.0831	0.0757	0.1646
K_{40}	—	0.1484	0.2067	−0.9359
K_{60}	—	—	−0.2837	15.64
K_{80}	—	—	1.5701	−207.7
K_{100}	—	—	—	2368.0
K_{120}	—	—	—	−15130.0
Error	0.3282	0.2531	0.2363	0.1437

D. Discussion of Results

The coefficients $\hat{I}_{lq}$ in the expansion of the normalized CCSD [Eq. (22)] for a semidiffuse field can be computed exactly (see appendix). These correct values are included in Tables 2 and 4 for comparison.

Although it is clear that firm quantitative conclusions cannot be drawn about the modal content of the test duct sound field from these results, the following points can be made:

1) The agreement between computed and exact coefficients in the case of synthetic input data is much better for choice 2 (axisymmetric terms) than for choice 1 (low-order terms) (see Tables 2 and 4). The CCSD in a semidiffuse field is in fact made up only of axisymmetric terms. This shows that an appropriate choice of terms in S_N is important.

2) If N is unreasonably large, although a fit can always be made, the results may not be meaningful. This is illustrated by the behavior of K_{10} in Table 3. As N is increased from 2 to 4, the change in K_{10} is about 20%; but as N is increased from 4 to 8, the change in K_{10} is about 350%. This limit on N, i.e., the truncation of the fitting series S_N, provides a resolution limit to the final estimate of modal power.

3) The presence of noise in real data undoubtedly affects the validity of the fitting procedure, as can be seen from Tables 3 and 5.

Given these provisos, however, the results presented here do indicate that analysis of data along these lines, using more sophisticated fitting procedures, could form the basis of a usable experimental technique for investigating the modal content of the sound field of a duct. This is illustrated by the good agreement between the computed and exact coefficient values for the synthetic input data given in Table 2.

V. Conclusion

In this paper, new theoretical results about the high-frequency behavior of sound in a duct have been presented. These results can be used as the basis for a new experimental technique for estimating the modal power distribution in the duct. The technique is designed to work at high frequencies, where attempts to resolve for individual modes are impractical. Preliminary results from an experiment using the new technique indicate that using as few as 12 microphone positions may yield a useful estimate of the modal power distribution, even at high frequency.

Appendix: Properties of Normalized CCSD in a Semidiffuse Field

This appendix is a summary of some new analytical results about the properties of the normalized CCSD function in a semidiffuse field. The results were used to derive 1) the ideal semidiffuse field CCSD plot shown in Fig. 4, 2) the synthetic input data set used to test the least-squares fitting procedure described in the main text, and 3) the analytically exact coefficients given for comparison in Tables 2 and 4.

Integral Expression for Normalized CCSD

In this section, a new integral expression for the normalized CCSD in a semidiffuse field $C(r,\theta,\phi)$ is given. It is straightforward to show, from Eq. (5) and standard Bessel function results,[10] that

$$C(r,\theta,\phi) = \tfrac{1}{2}\pi \int_0^{2\pi} du \int_0^{\pi/2} dv\ \sin v\ \exp[ikr\cos\theta\ \cos v + ikr\sin\theta\ \sin v\ \cos(\phi-u)] = \int_0^{\pi/2} dv\ \sin v\ \exp(ikr\cos\theta\ \cos v) J_0(kr\sin\theta\ \sin v) \quad \text{(A1)}$$

Note that C is independent of ϕ.

It can be shown, from the standard results

$$\frac{d}{dx} J_0 = -J_1(x) \quad \text{(A2)}$$

$$\frac{d}{dx} J_1(x) = J_0(x) - \frac{1}{x} J_1(x) \quad \text{(A3)}$$

that

$$i\frac{\mathrm{d}}{\mathrm{d}\theta}\left[\sin v\ \exp(ikr\cos\theta\ \cos v)J_0(kr\sin\theta\ \sin v)\right]$$

$$=\frac{\mathrm{d}}{\mathrm{d}v}\left[\sin v\ \exp(ikr\cos\theta\ \cos v)J_1(kr\sin\theta\ \sin v)\right] \quad \text{(A4)}$$

It follows from Eqs. (A1) and (A4) that

$$\frac{\mathrm{d}C}{\mathrm{d}\theta}=-iJ_1(z\sin\theta) \quad \text{(A5)}$$

Hence

$$C(r,\theta)=C(r,0)-i\int_0^\theta \mathrm{d}\theta J_1(z\sin\theta) \quad \text{(A6)}$$

where[8]

$$C(r,0)=j_0(kr)+[i(1-\cos kr)]/kr \quad \text{(A7)}$$

Equation (A6) is a more useful form for computation than Eq. (A1). It was used to derive the synthetic data mentioned in the main text.

Expansion for Normalized CCSD

In this section an expression of the form of Eq. (22) for the normalized CCSD in a semidiffuse field is discussed. Using the results[10] that

$$\int_0^1 P_l(x)\,\mathrm{d}x=\frac{(-)^r(2r)!}{2^{2r+1}(r+1)!r!} \quad \text{(A8)}$$

if $l=2r+1$ with r integer, and that the integral is zero otherwise, the coefficients $\hat{I}_{lq}$ in the expansion of the form (22) for C in a semidiffuse field are

$$\hat{I}_{lq}=1/(4\pi)^{1/2} \qquad \text{if } l=0, q=0 \quad \text{(A9)}$$

$$=\frac{(-)^r(4r+3)^{1/2}(2r)!}{(4\pi)^{1/2}2^{2r+1}(r+1)!r!} \qquad \text{if } l=2r+1,\ q=0$$

$$=0 \qquad \text{otherwise} \quad \text{(A10)}$$

These coefficients are the exact coefficients given for comparison in Tables 2 and 4.

Acknowledgment

S. M. Baxter acknowledges the joint financial support of the Science and Engineering Research Council and the National Gas Turbine Establishment through a CASE award.

References

[1] Waterhouse, R. V., "Noise Measurements in Reverberant Rooms," *Journal of the Acoustical Society of America,* Vol. 54, 1973, pp. 931-934.

[2] Baxter, S. M., "Acoustic Modal Power Distribution in a Duct at High Frequencies," Institute of Sound and Vibration Research, Southampton University, Tech. Rept. 111, 1981.

[3] Morse, P. M. and Feshbach, H., *Methods of Theoretical Physics,* McGraw-Hill, New York, 1953, pp. 1432-1512.

[4] Bart, G. C. J., "Spatial Cross-Correlation in Anisotropic Sound Fields," *Acustica,* Vol. 28, 1973, pp. 45-49.

[5] Cox, H., "Spatial Cross-Correlation in Arbitrary Noise Fields with Applications to Ambient Sea Noise," *Journal of the Acoustical Society of America,* Vol. 54, 1973, pp. 1289-1301.

[6] Morrow, C. T., "Point-to-Point Correlation of Sound Pressures in Reverberant Chambers," *Journal of Sound and Vibration,* Vol. 16, 1971, pp. 29-42.

[7] Blake, W. K. and Waterhouse, R. V., "The Use of Cross-Spectral Density Measurements in Partially Reverberant Sound Fields," *Journal of Sound and Vibration,* Vol. 54, 1977, pp. 589-599.

[8] Cook, R. K., Waterhouse, R. V., Berendt, R. D., Edelman, S., and Thompson, M. C., "Measurement of Correlation Coefficients in Reverberant Sound Fields," *Journal of the Acoustical Society of America,* Vol. 27, 1955, pp. 1072-1077.

[9] Wyld, H. W., *Mathematical Methods for Physics,* Benjamin Inc., Reading, Mass., 1976, pp. 74-121.

[10] Abramowitz, M. and Stegun, I. A., *Handbook of Mathematical Functions,* Dover, New York, 1972, pp. 355-434.